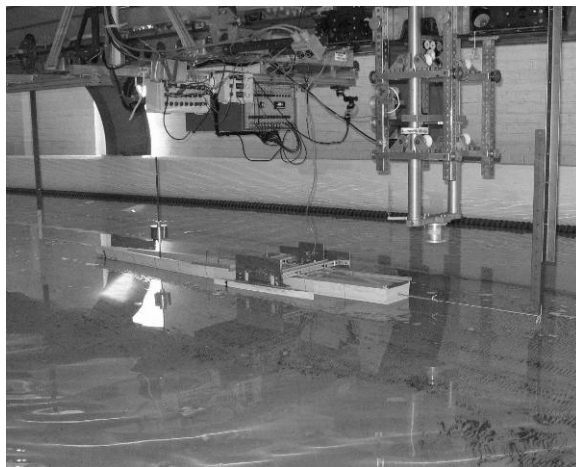


# Experimental analysis of roll damping of a trimaran with varying side hull stagger and transverse spacing

A. S. Onas, M.Sc., Doctoral Candidate, Stevens Institute of Technology, Hoboken, USA  
R. Datla, Ph.D., Research Associate Professor, Stevens Institute of Technology, Hoboken, USA



*This paper summarizes a series of roll damping experiments conducted at Davidson Laboratory at Stevens Institute of Technology as a preliminary investigation in the hydrodynamics of a high-speed displacement frigate-type trimaran. Roll decay tests in calm water at zero and forward-speed were carried-out with a 1:125 scale model. The setup featured a special apparatus for changing the side hull position at transverse spacing to beam ratios of 0.31, 0.5, 0.7 and longitudinal stagger to length ratios of 0.72, 0.77 and 0.82. The trimaran response in beam seas was investigated in regular waves. An assessment of roll damping is presented, which will be followed in a later treatment by seakeeping numerical simulations. The final objective of the work is to evaluate the contribution of viscous roll damping, which unlike roll radiation damping cannot be numerically computed using potential flow theory. Roll resonance such as parametric roll instability in head seas can be predicted with knowledge of the viscous roll damping magnitude. The experimental results could be used to check the suitability of the uncoupled 1 DOF roll damping mathematical model. Such formulation was applied with limited success on trimarans due to the highly non-linear characteristic of their roll motion thereby producing high scatter in the roll damping coefficients.*

## KEY WORDS

Roll damping; free roll decay; roll response amplitude operator; roll extinction curve; parametric roll.

## NOMENCLATURE

$a$  – Distance from CG to the knife edge contact  
 $A_{44}$  – Added mass moment of inertia for roll motion  
 $B_{44}$  – Coefficient of total roll damping moment  
 $B_{44,1-3}$  – First, second, third order coefficient of roll damping moment  
 $B_e$  – Equivalent coefficient of roll damping moment  
 $C_{44}$  – Coefficient of roll restoring moment  
 $GM$  – Transverse metacentric height  
 $I_{xx}$  – Mass moment of inertia for rolling  
 $I'_{xx}$  – Virtual mass moment of inertia for rolling  
 $k_{xx}$  – Roll radius of gyration  
 $k'_{xx}$  – Virtual roll radius of gyration  
 $RAO$  – Response Amplitude Operator  
 $t$  – time  
 $T$  – roll swing test period of oscillation  
 $VCG$  – Vertical center of gravity

$t/B$  – ratio of side hull/main hull separation to main hull beam  
 $l/L$  – ratio of distance (stem to side hull midships) to main hull length  
 $\omega_0$  – undamped natural frequency of the model

$\phi, \dot{\phi}, \ddot{\phi}$  – Roll angle, roll velocity and roll acceleration

$\Delta$  – Displacement;  $\Delta'$  – Virtual Displacement

## INTRODUCTION

The trimaran concept has gained popularity in the ship industry due to its ability to reduce wave making resistance at moderate speeds by using a very slender main hull, while compensating and providing for the additional transverse stability with its side hulls or outriggers. Unlike a monohull, the trimaran gives greater flexibility to the designer in allowing control over ship motions by simply adjusting the location of the side hulls and hence changing the roll natural frequency. Undesirable roll accelerations can now be controlled directly through side hull design. In the case of a traditional vessel, the naval architect would only be able to make changes to the monohull's

dimensions, which can now be optimized for resistance and left almost intact in the rest of the design process. Resistance characteristics of the trimaran under investigation were extensively studied at Davidson Laboratory during the past two years at two separate scales, namely 1:80 and 1:125. Research on optimization of the outrigger locations that generate the lowest resistance have just been completed. The second part of the project is to analyze the roll damping characteristics of the trimaran as part of a more extensive seakeeping investigation. This will allow identification of configurations susceptible to the resonance phenomenon of interest called parametric roll. Such instability produces increasingly large roll angles when the instantaneous restoring lever ( $GZ$ ) varies significantly in waves, which can lead to loss of deck cargo or even capsizing (Kat et al, 2002). It could also occur as a result of head wave excitation energy input into the pitch or heave motions, which may be transferred to the roll motion due to nonlinear coupling between the modes (Oh et al, 2000). The latter instability is called autoparametric resonance. Both are mainly known to occur on vessels with pronounced bow flare, flat transom and reduced parallel mid-body such as containerships and small fishing boats. On trimarans, the danger for parametric roll arises from the existence of side hulls and the abrupt variation in transverse stability they may cause when the ship encounter head waves at a frequency of twice the natural roll frequency. Knowledge of roll damping is critical if accuracy is to be expected from time domain potential flow ship motion simulations, which can only predict the radiation damping component of total roll damping.

#### MODEL DESCRIPTION

The model used in the roll damping experiments (Fig. 1) is a 1:125 scale high-speed displacement frigate-type ship. The trimaran lines plan (Fig. 2) was provided by the Center for Innovation in Ship Design at Naval Surface Warfare Center, Carderock Division (NSWCCD). The particulars of the full scale and model are shown in Table 1. The test model was manufactured at Webb Institute and consists of a main hull and two side hulls, with each side-hull being approximately 3% of the main hull displacement.

Table 1. Full-scale and model particulars

Full-Scale		1:125 Scale Model	
<b>Center Hull</b>		<b>Center Hull</b>	
Length	268.3 m	Length	2.14 m
Beam	25.9 m	Beam	0.21 m
Depth	17.4 m	Depth	0.14 m
Draft	9.0 m	Draft	0.07 m
		Wetted Area	0.48 m <sup>2</sup>
<b>Side Hull</b>		<b>Side Hull</b>	
Length	77.0 m	Length	0.61 m
Beam	3.8 m	Beam	0.03 m
Depth	11.5 m	Depth	0.09 m
Draft	7.1 m	Draft	0.06 m
		Wetted Area	0.06 m <sup>2</sup>
<b>Displacement</b>	32,200 MT		16.20 kgs
<b>Design Speed</b>	32 knots		

The model was fitted with an apparatus that allowed changes in the side-hull transverse and longitudinal locations (Fig. 3a). The apparatus was made with aluminum bar and resin-coated plywood to make it water-proof. No bilge keels or fins were fitted to the model.



Fig. 1 Photograph of trimaran model with side-hull apparatus

#### TEST MATRIX

The model was configured, ballasted and tested based on a matrix that includes nine side-hull longitudinal stagger and transverse spacing locations (Table 2).

Table 2. Model roll-damping test matrix

CONFIG.	GM		t/B	l/L	FRD-ZS	FRD-FS	RAO-BS
	mm	in					
A	44	1.73	0.31	0.72	X	X	X
	30	1.17			X	X	
	16	0.63			X	X	
B	44	1.72	0.31	0.77	X	X	
	28	1.12			X	X	
	14	0.55			X	X	
C	44	1.72	0.31	0.82	X	X	X
	27	1.07			X	X	
	14	0.57			X	X	
D	73	2.89	0.50	0.72	X	X	X
	56	2.21			X	X	
	43	1.69			X	X	
E	73	2.88	0.50	0.77	X	X	
	54	2.13			X	X	
	45	1.75			X	X	
F	73	2.86	0.50	0.82	X	X	X
	58	2.28			X	X	
	44	1.75			X	X	
G	107	4.22	0.70	0.72	X	X	X
	94	3.68			X	X	
	79	3.13			X	X	
H	108	4.26	0.70	0.77	X	X	
	92	3.60			X	X	
	82	3.24			X	X	
	44	1.72			X		
I	108	4.27	0.70	0.82	X	X	X
	91	3.59			X	X	
	81	3.17			X	X	
	44	1.72			X		

This allowed an investigation of roll damping as a function of side hull locations and loading condition. The non-dimensional ratios  $t/B$  and  $l/L$  are shown in Fig. 3b. The  $VCG$  and roll radius of gyration were measured with a swing test.  $GM$  was computed using Rhino Marine hydrostatics and the measured  $VCG$ .

The following tests have been carried-out, as shown in Table 2. The nine side hull model configurations are shown in Fig. 3a.

- a) Free-Roll Decay at Zero Speed (FRD-ZS)
- b) Free-Roll Decay at Forward Speed (FRD-FS)
- c) Roll Response in Beam Seas at zero speed (RAO-BS)

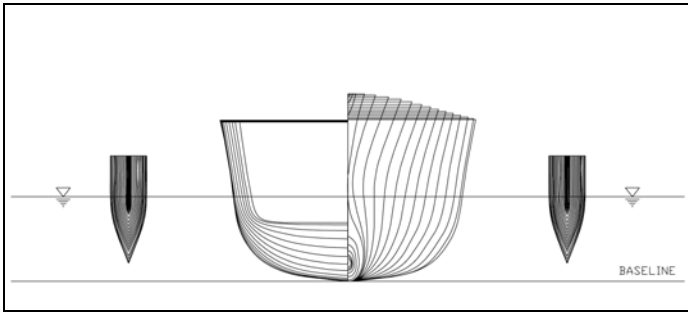


Fig. 2 Lines plan for trimaran configuration B.

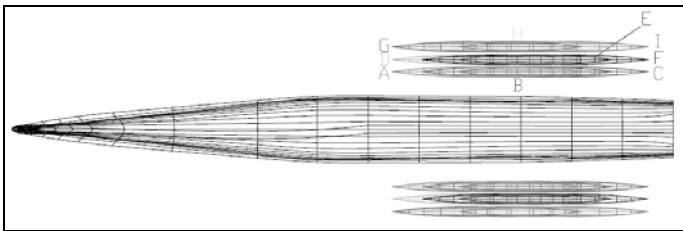


Fig. 3a Trimaran plan view showing the nine configurations

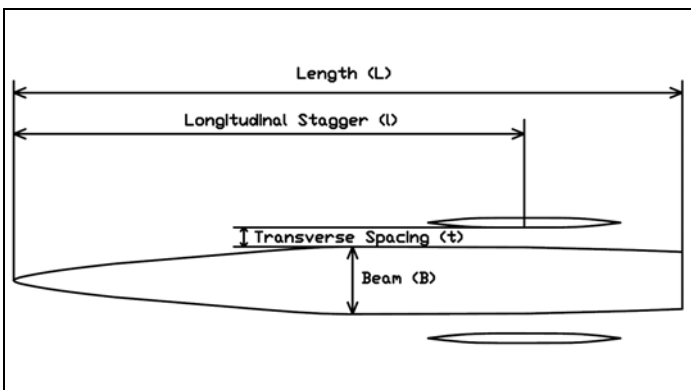


Fig. 3b Trimaran transverse spacing and longitudinal stagger

## FACILITIES

The model tests were carried-out in the high-speed towing tank at Davidson Laboratory, Stevens Institute of Technology, Hoboken, NJ, USA. The particulars of the test facility are:

Length	: 320 ft (97.5 m)
Breadth	: 16 ft (4.9 m)
Depth	: 8 ft (2.4 m)
Monorail carriage maximum speed	: 100 ft/sec (30.5 m/sec)

## DATA MEASUREMENTS

The model was equipped with a Systron Inertial Gyro Chip II, which measured roll velocity in dynamic conditions at sampling rates of 150 Hz. Gyros are affected by data drifting, which is generally amplified by integration of angular velocity. This effect was minimized by normalizing the output signal before final processing. This solution provided reasonable results and it was easy to implement. Gyros are also much cheaper alternatives to direct optical measurement systems.

Noise was eliminated even though filtering becomes an issue when angular velocity derivative is needed. The fluctuations about the mean of roll angular velocity have been pre-processed with a least-squared Savitzky-Golay filtering method from

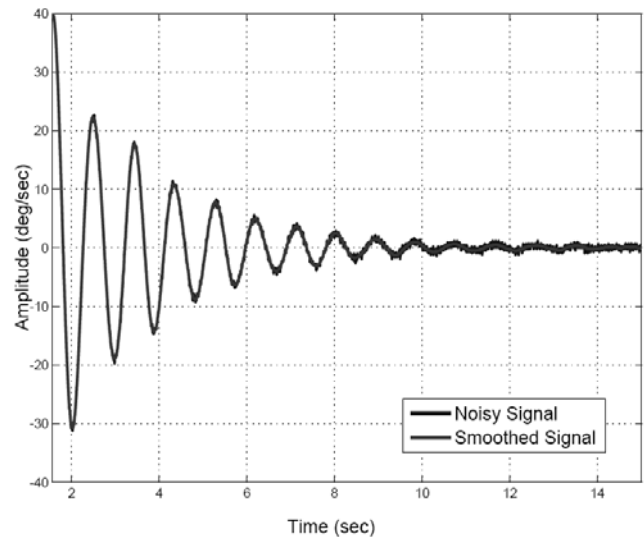


Fig. 4 Smoothed data after applying the Savitzky-Golay filter

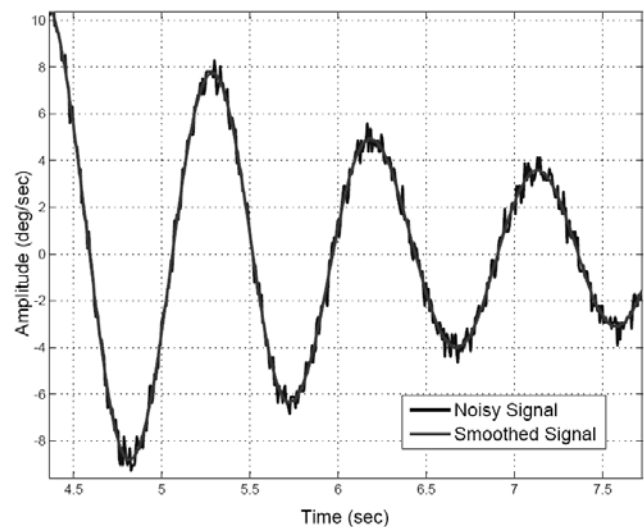


Fig. 5 Smoothed data detail that shows smoothing and noise

Matlab by using the command **sgolayfilt**. The smoothed result detail is shown in Fig. 5 with the angular velocity first plotted using gyro sensor data and then smoothed with the filter. The filter frame is tuned to match the amplitude of the noisy signal. The resulting signal was then integrated using an approximation of the cumulative integral based on the trapezoidal method.

## EXPERIMENTS

The challenge in model testing is to find a compromise between having an experimental setup that allows measurement of physical parameters of interests and the simplifications employed in the process that make the test possible.

When carrying-out roll decay experiments we assume that motions in other degrees of freedom namely, surge, sway, heave, pitch and yaw do not affect the roll motion. This may seem to be a major simplification of our problem. However, we find quickly that it is not unreasonable at all if we consider the following:

- Surge, sway and yaw had little fluctuations in the setup for Free Roll Decay at zero speed shown in Fig. 6. The two sets of springs fore and aft were placed close to the center of rotation in roll and set 90 degrees apart almost parallel to the water surface. The strings position and tension were “tuned” to limit surge and sway and have a limited and minimal impact on roll response.

- Heave motion generated by the initial heel given to the model at the beginning of each run had small amplitude and decayed quickly (Fig. 7, 8). It had some influence only during the first or second roll decay oscillations, which are normally removed from the final analysis.

- Pitch motion had some influence only for the aft most trimaran configurations, namely *C*, *F* and *I* (Fig. 7, 8). It too, as the heave motion, had small amplitude although it decayed slower than the heave motion.

The second assumption is related to the test conditions and the characteristics of the roll motion itself. The towing tank walls had little influence on the model, due to the orientation of the latter, which is perpendicular to the tank walls. Any waves radiated from the hull will travel away from the model port and starboard and will reflect back long after the test measurements were made.

As indicated above, the free roll decay tests were carried-out by heeling the model to an initial angle. This was done by slowly pushing the port outrigger downward just below its buoyant top side and then quickly releasing it. This procedure proved to be as accurate as the more traditional removal of weight from one side of the model and was found to be easier to implement, especially at forward speed. Both methods will generate heave and pitch and the only known way by the authors to eliminate their effect is by using a captive model, which has its own issues

associated with the need of precisely locating the center of gravity and center of rotation.

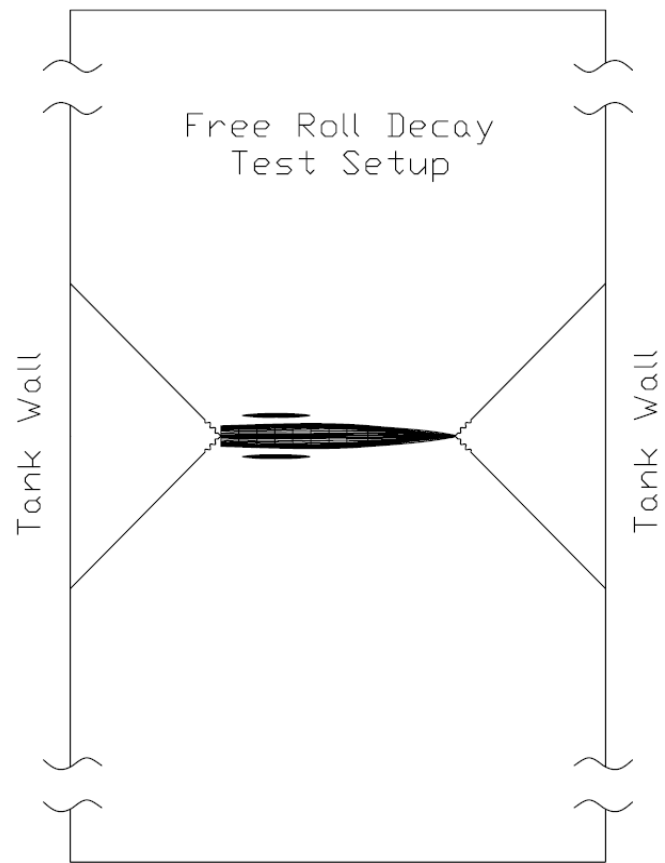


Fig. 6 Model setup for Free Roll Decay at zero speed

This represents an initial value problem, with the excitation moment in the uncoupled equation of motion for roll being zero (see Eq. 4).

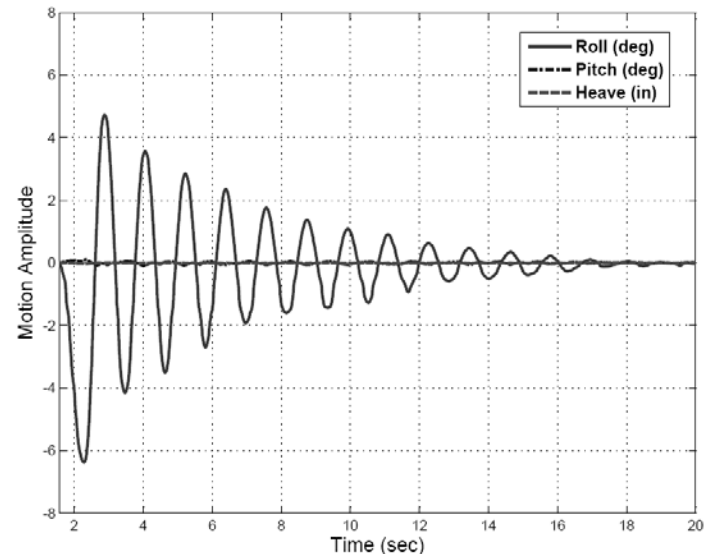


Fig. 7 Heave and Pitch coupling during a free roll decay test

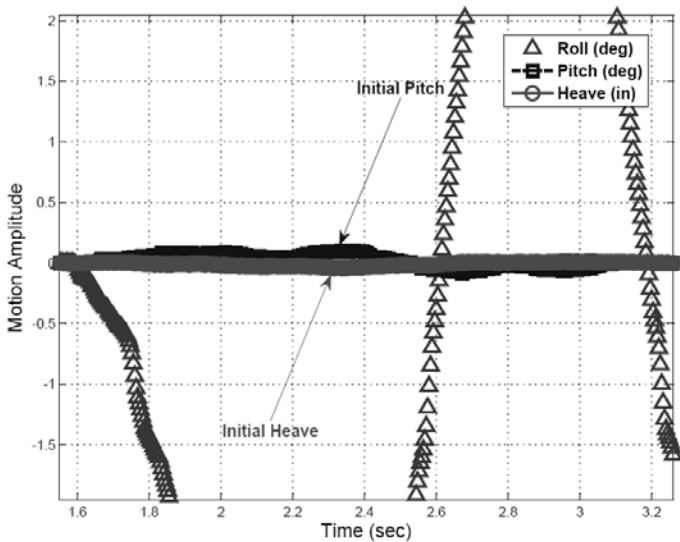


Fig. 8 Initial pitch and heave amplitudes and their decay

As mentioned earlier, the resulting motion in other degrees of freedom and their coupling with the roll motion, such as heave and pitch were negligible, as shown in Fig. 8.

#### FREE ROLL DECAY AT ZERO SPEED

All trimaran configurations have been tested at three separate loading conditions, based on a low, mid and high VCG, which yielded three corresponding GM values. Configurations *G*, *H* and *I* have been tested at an additional loading condition, which corresponded with an even lower GM. This can provide a comparison of all nine configurations at the same metacentric height of  $44 \pm 1$  mm.

Each set of three plots in Fig. 9-17 represent the free roll decay time histories at zero speed for each loading condition, starting with stern inward and going forward outward. The plots show the effect of transverse location of the side hulls on the roll damping moment and roll natural frequency, which increase as the side hull separation to beam ratio increases. This is shown starting with the stern stagger, mid and forward stagger for each of the transverse location. We investigate in a similar manner the effect of longitudinal stagger on the trimaran roll damping characteristics. Changes in the longitudinal location of the side hulls at the same transverse position seem to slightly affect the damped natural roll frequency only in the second half of each roll decay time history for the three sets shown in Fig. 18-20. The authors suspect this is generated by a small shift in LCG and roll radius of gyration due to longitudinal stagger change, which may have not been perfectly balanced by the weight shift within the model. It should be noted here that the initial angle of inclination of to model during the decay tests varied due to the transverse separation, which reduced the initial amplitude as the  $t/B$  ratio increased. Since the damped roll frequency depends on amplitude, we expect some difference in the magnitude of the natural roll period. However, as will be shown in the final analysis in Fig. 38-40, the average fluctuation in damped natural period per decay is about 5 %.

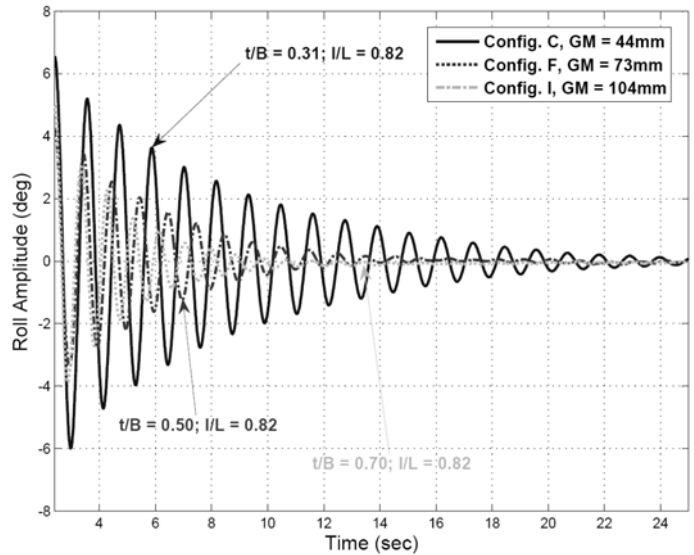


Fig. 9 Roll decay time history runs 175/190/194, low VCG

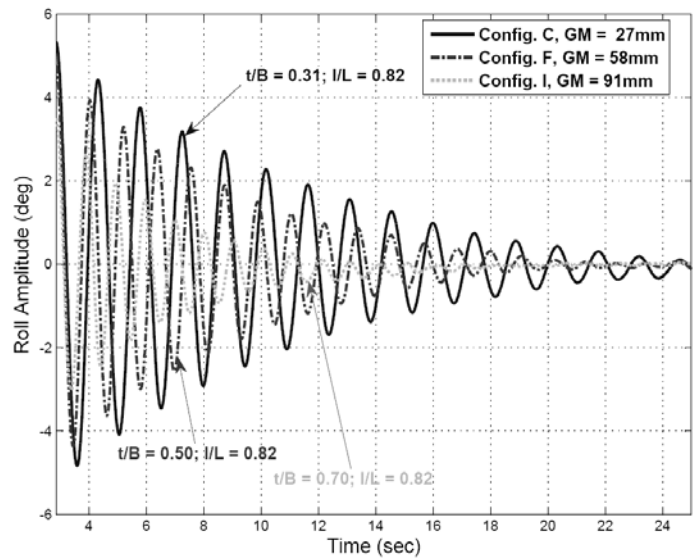


Fig. 10 Roll decay time history runs 177/186/197, mid VCG

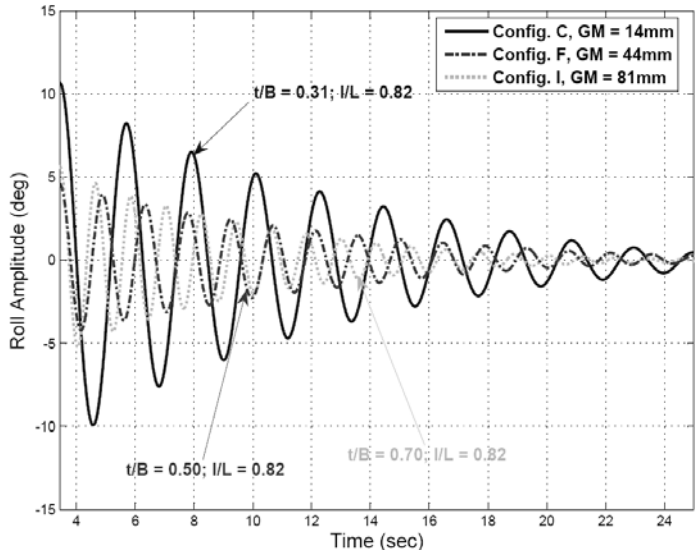


Fig. 11 Roll decay time history runs 180/185/200, high VCG

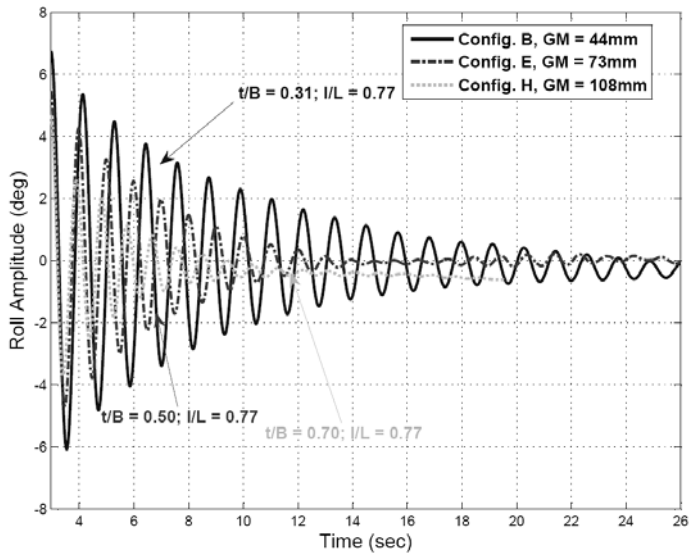


Fig. 12 Roll decay time history runs 171/139/129, low *VCG*

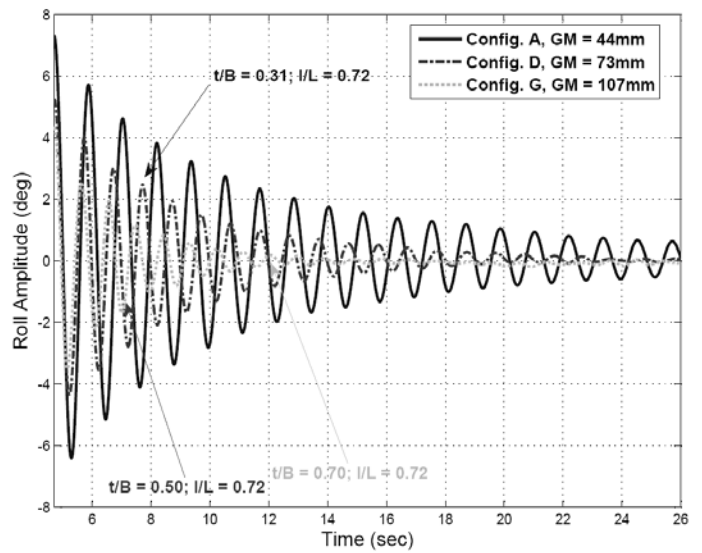


Fig. 15 Roll decay time history runs 73/98/101, low *VCG*

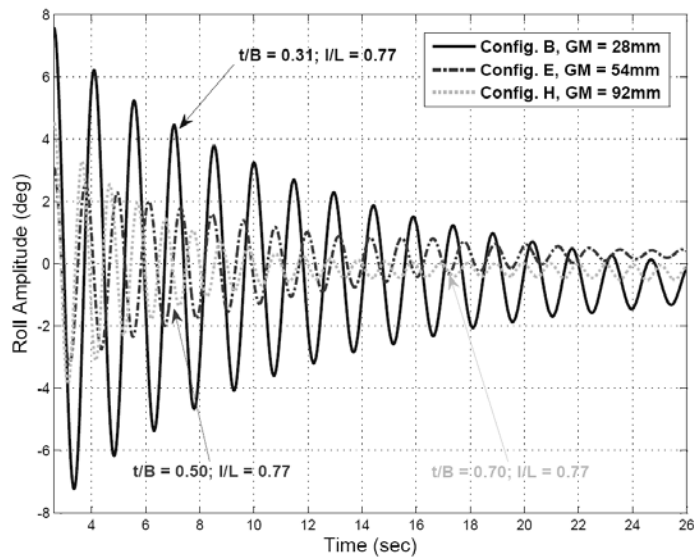


Fig. 13 Roll decay time history runs 168/153/127, mid *VCG*

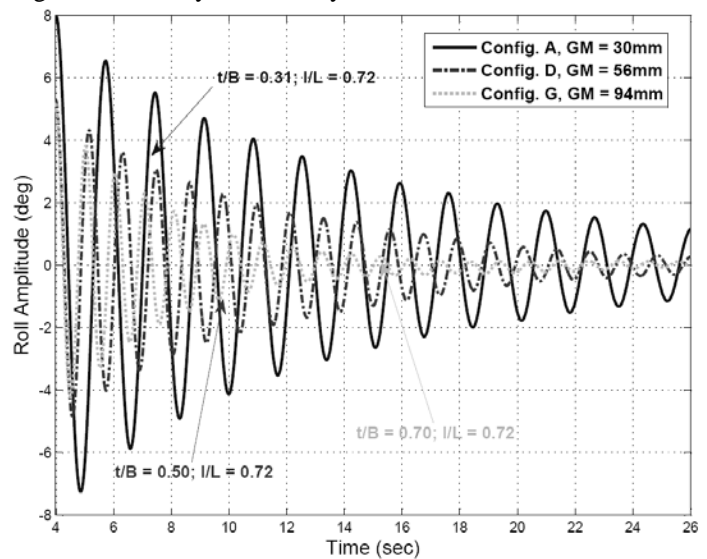


Fig. 16 Roll decay time history runs 74/95/106, mid *VCG*

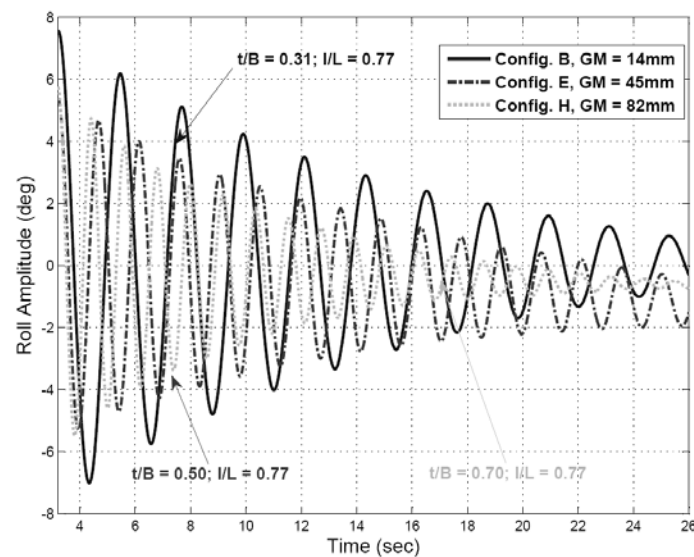


Fig. 14 Roll decay time history runs 166/161/131, high *VCG*

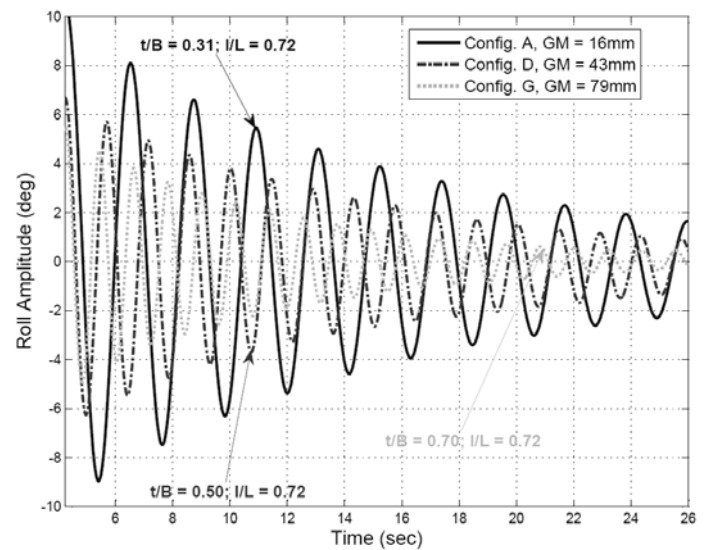


Fig. 17 Roll decay time history runs 89/92/109, high *VCG*

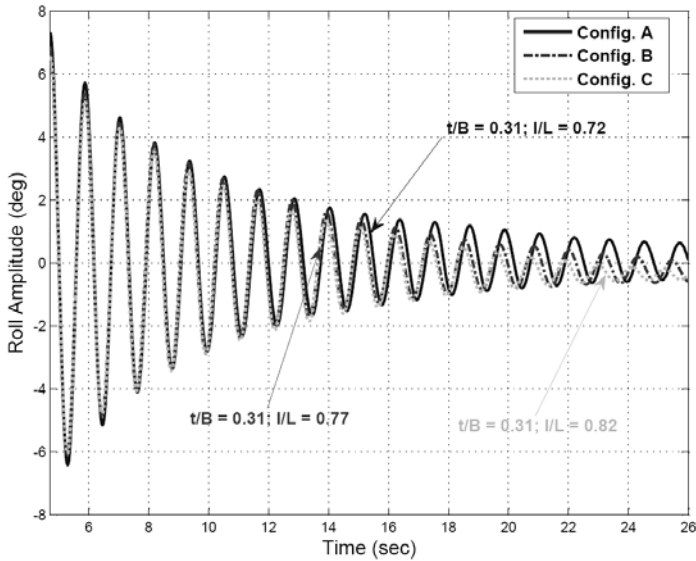


Fig. 18 Roll decay time history runs 73/171/175,  $GM = 44\text{mm}$

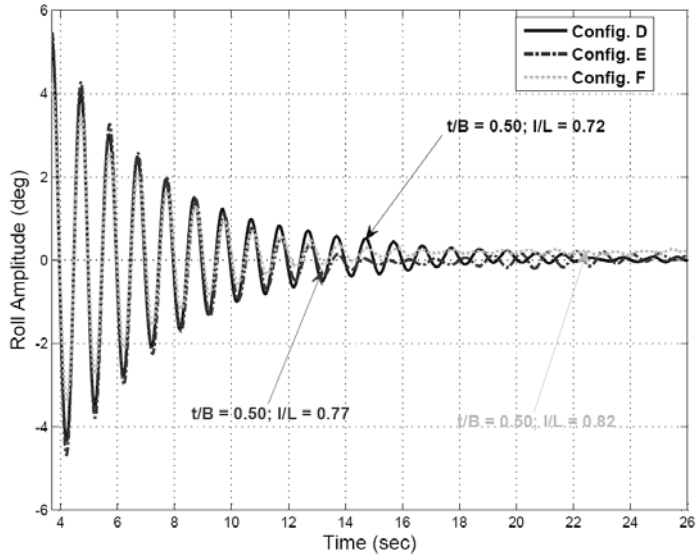


Fig. 19 Roll decay time history runs 98/139/190,  $GM = 44\text{mm}$

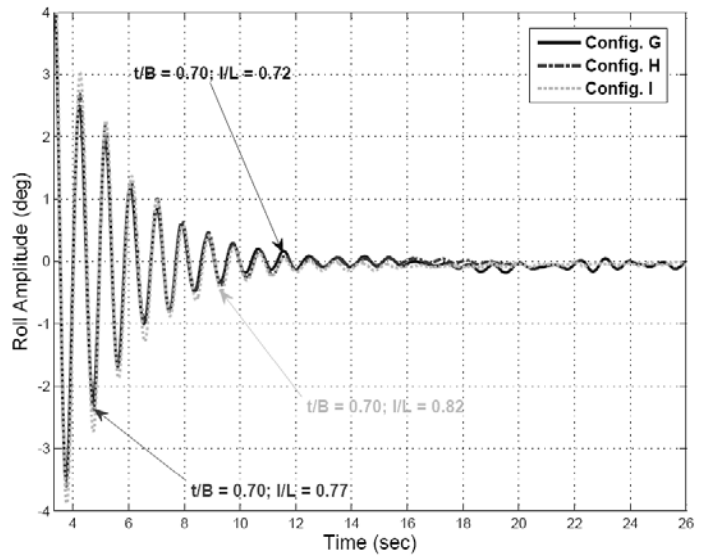


Fig. 20 Roll decay time history runs 101/129/194,  $GM = 44\text{mm}$

### FREE ROLL DECAY AT FORWARD SPEED

The test setup at forward speed consisted of a rig attached to the tank monorail carriage, as shown in Figure 21. It was designed to tow and provide controllability to the model. The tests were performed at three different Froude numbers,  $F_n = 0.16, 0.24$  and  $0.32$  respectively.

The roll angle inclination was initiated, as in the free roll decay tests at zero speed, by applying a roll moment to the port side outrigger, which was then quickly removed to allow the roll motion decay while measurements were taken using the gyro sensor and processed by a data acquisition system.

The roll decay curves shown in Fig. 22-30 are for each of the nine model configuration at the three different Froude numbers at which the model was ran through the towing tank.

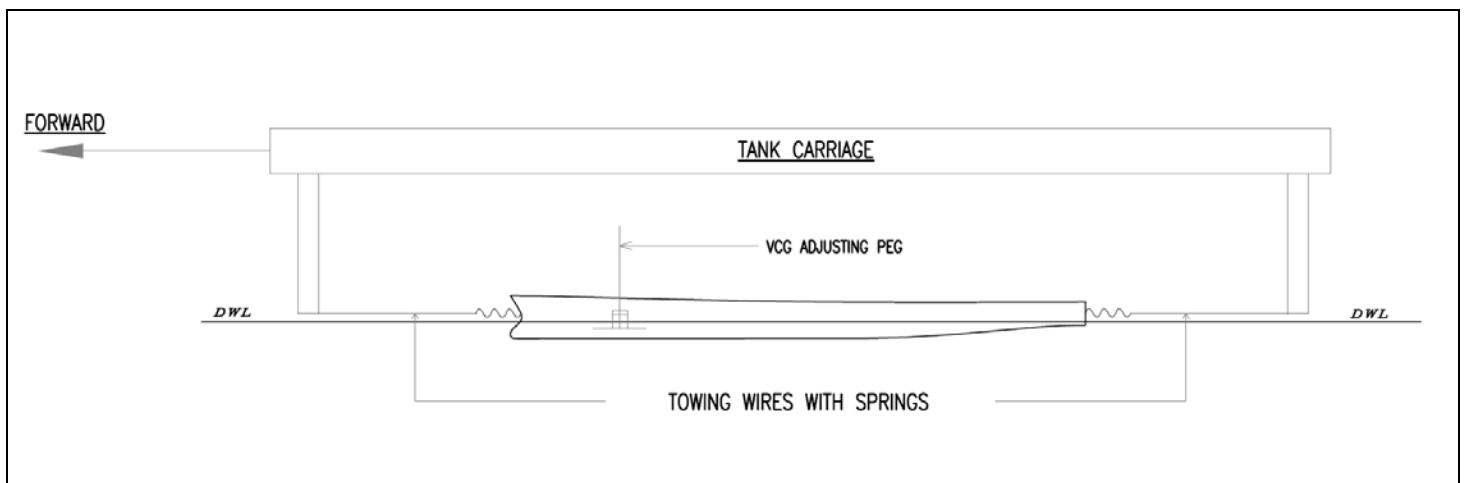


Fig. 21 Free-roll decay rig showing monorail tank carriage towing the model at forward speed using stem/stern wires with springs

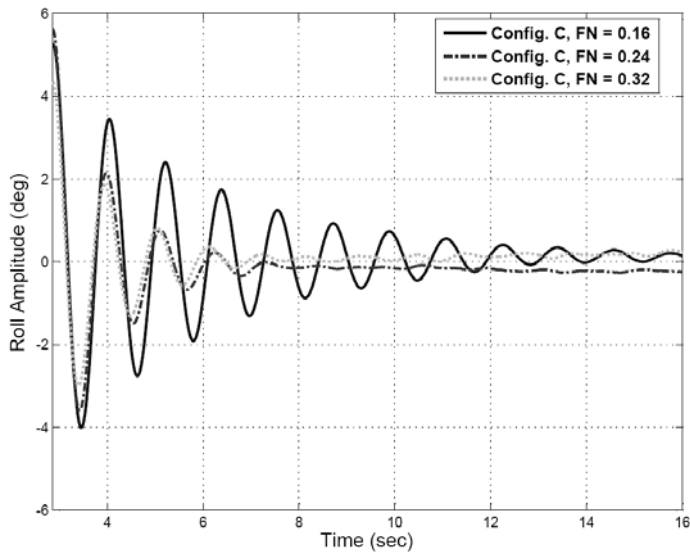


Fig. 22 Roll decay time history runs 286/288/291,  $GM = 44$ mm

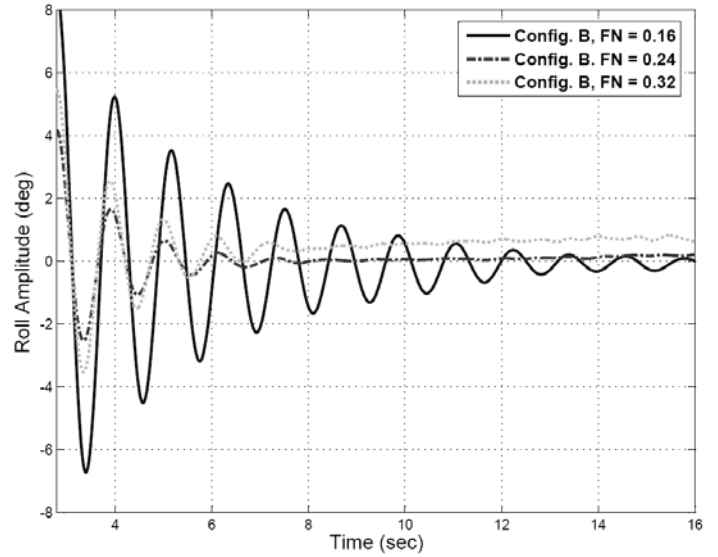


Fig. 25 Roll decay time history runs 295/296/301,  $GM = 44$ mm

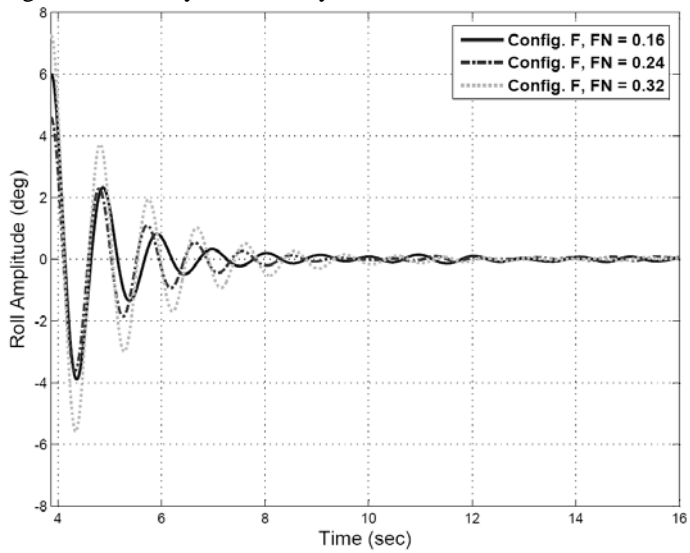


Fig. 23 Roll decay time history runs 233/234/239,  $GM = 73$  mm

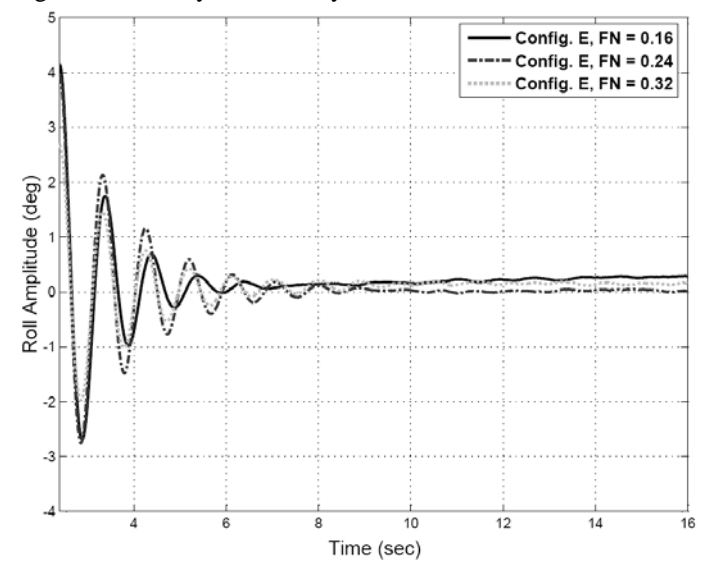


Fig. 26 Roll decay time history runs 331/333/335,  $GM = 73$ mm

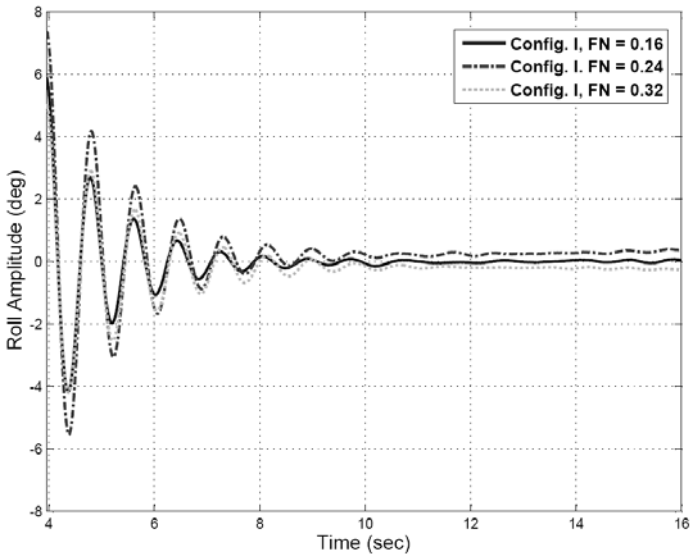


Fig. 24 Roll decay time history runs 233/234/239,  $GM = 108$  mm

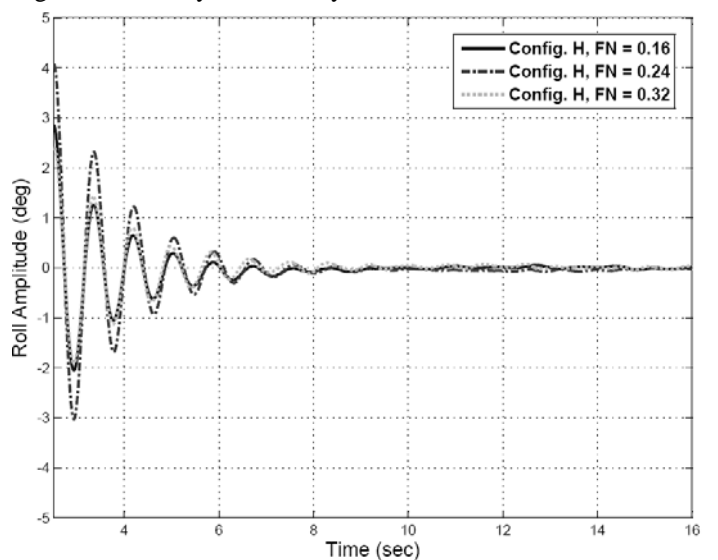


Fig. 27 Roll decay time history runs 336/338/340,  $GM = 108$ mm



## ROLL RESPONSE IN BEAM SEAS

The model was setup in the same configuration used for free roll decay test at zero speed (see Fig. 6). Based on the roll damped natural frequency observed during the decay tests at zero speed, the model roll response in beam regular waves was analyzed for six of the nine configurations each at its high GM loading condition. Configurations B, E and H were skipped as it was expected that longitudinal stagger would not have a significant influence on roll response.

For the roll motion, the Roll Response Amplitude Operator (RAO) is:

$$RAO(roll) = \frac{\phi_0}{k\eta} \quad (1)$$

where:

$\phi_0$  - roll amplitude

$k$  - wave number

$\eta$  - wave amplitude

The roll response operator in Eq. (1) provides important information about ships' behavior in beam waves. It is well known that close to the ship's damped natural roll frequency, there will be an amplification of the roll response, as shown by Belenky & Sevastianov (2007) in Eq. (2).

$$\phi_0 = \phi_{\max} = \frac{\alpha_E}{2\nu\omega_\phi} \quad (2)$$

$$\omega = \omega_\phi \quad (3)$$

where:

$\alpha_E$  - amplitude of the wave force

$2\nu$  - damping coefficient per unit total mass moment of inertia

$\omega$  - wave frequency

$\omega_\phi$  - model damped roll natural frequency

When the beam wave frequency is within the range of the ship's damped natural roll frequency, the trimaran is expected to exhibit the largest roll angles of inclination, which will be further magnified for lower values of damping coefficient.

The roll response for six out of nine trimaran configurations is shown in Fig. 31. Configurations B, E and H were skipped as it was expected that longitudinal stagger would not have a significant influence on roll response. It can be seen in the plot below that transverse spacing has the most impact on roll RAO, as expected. The response results will be compared in a later treatment with computer prediction of RAO obtained by using experimentally derived roll damping coefficients.

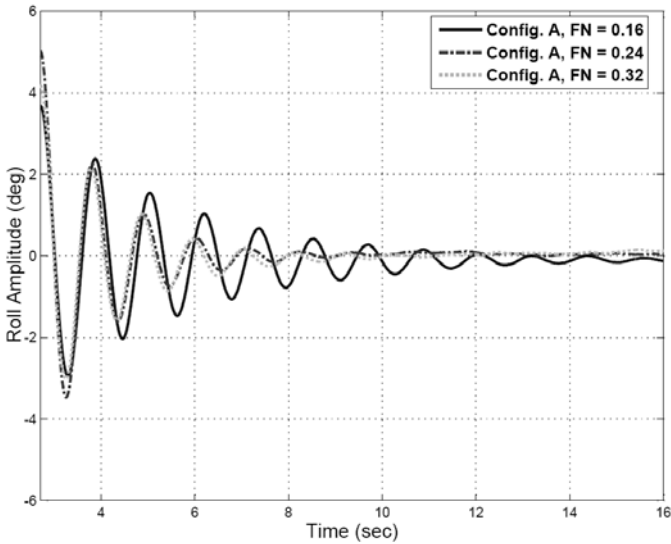


Fig. 28 Roll decay time history runs 406/412/414,  $GM = 44\text{mm}$

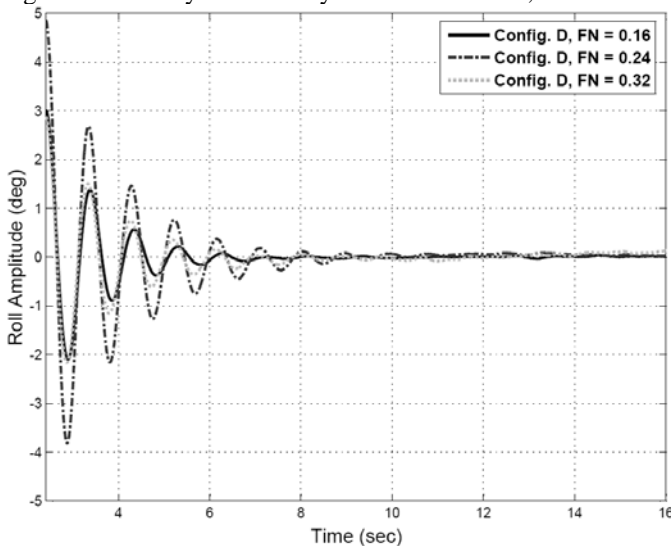


Fig. 29 Roll decay time history runs 331/333/335,  $GM = 73\text{mm}$

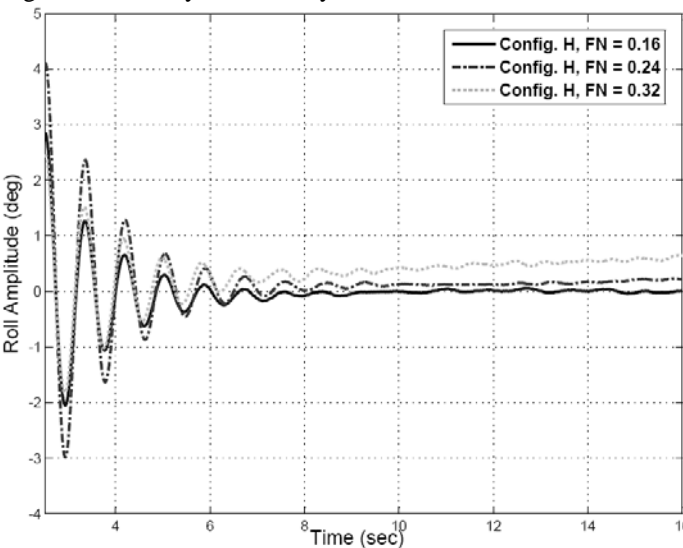


Fig. 30 Roll decay time history runs 336/338/340,  $GM = 108\text{mm}$

## Webb Trimaran Roll Response in Regular Beam Waves

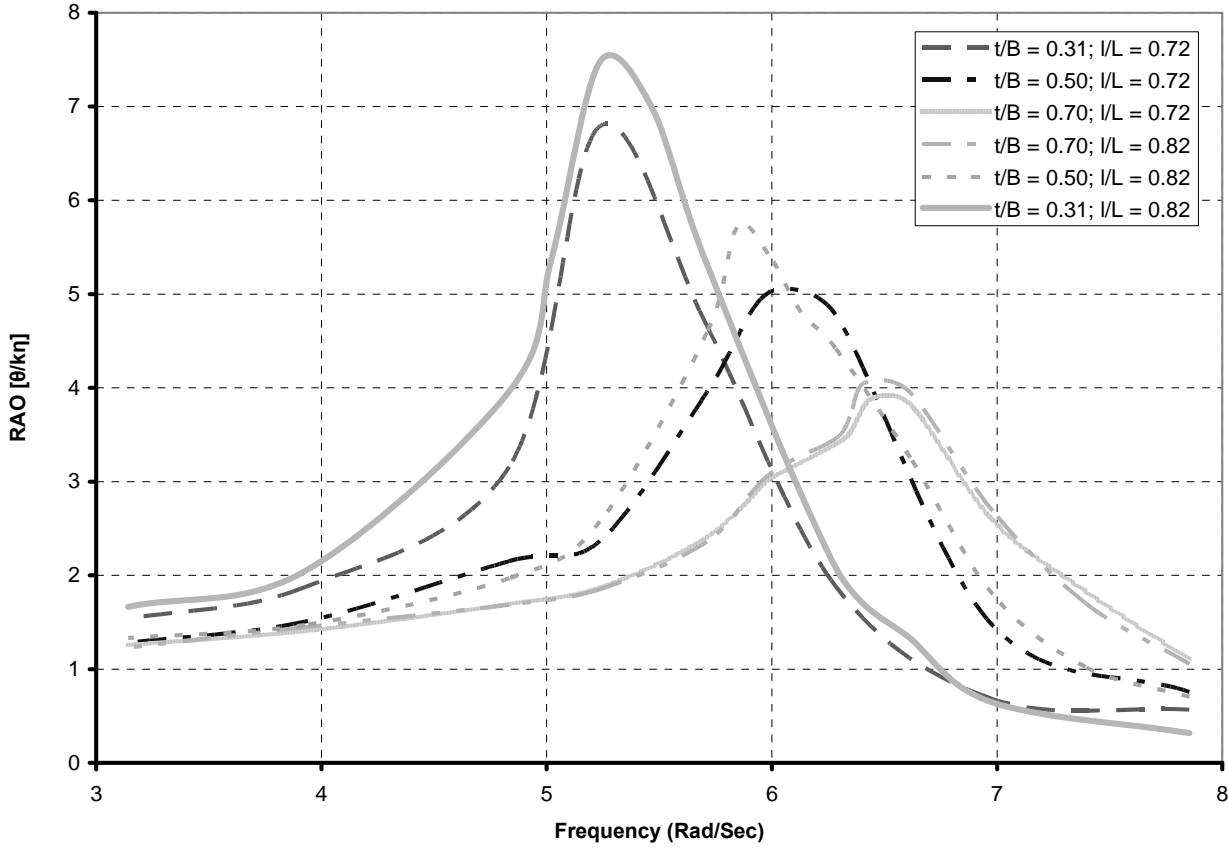


Fig. 31 Trimaran roll response in regular beam waves for fore/aft – inboard/outboard side hull configurations

### ROLL DAMPING THEORY

This analysis makes use of the aforementioned fact that no significant coupling of roll with motions in other degrees of freedom will occur. The total roll damping is evaluated using the one-degree-of-freedom equation of roll motion:

$$(I_{xx} + A_{44})\ddot{\phi} + B_{44}(\phi)\dot{\phi} + \Delta GZ(\phi) = 0 \quad (4)$$

The restoring moment can be written as a coefficient multiplied by the roll angle and the equation of motion becomes:

$$(I_{xx} + A_{44})\ddot{\phi} + B_{44}(\phi)\dot{\phi} + C_{44}(\phi)\phi = 0 \quad (5)$$

The non-linear damping term is expressed as a cubic polynomial of the following form:

$$B_{44}(\phi)\dot{\phi} = B_{44,1}\dot{\phi} + B_{44,2}\dot{\phi}|\dot{\phi}| + B_{44,3}\dot{\phi}^3 \quad (6)$$

After dividing by virtual mass moment of inertia, we can write the equation of roll motion using a non-linear roll damping model, as follows:

$$\ddot{\phi} + 2\nu\dot{\phi} + \alpha\dot{\phi}|\dot{\phi}| + \beta\dot{\phi}^3 + \gamma\phi = 0 \quad (7)$$

$$\nu = \frac{B_{44,1}}{2(I_{xx} + A_{44})}; \alpha = \frac{B_{44,2}}{I_{xx} + A_{44}}; \beta = \frac{B_{44,3}}{I_{xx} + A_{44}} \quad (8)$$

$$\gamma = \frac{C_{44}(\phi)}{(I_{xx} + A_{44})} \quad (9)$$

The trimaran under investigation is fitted with wall-sided outriggers without hunches, which do not produce significant changes in the buoyancy at angles below 10 degrees. At such angles of inclination, the restoring moment coefficient can be written as shown in Eq. (10):

$$\gamma = \omega_0^2 = \frac{C_{44}}{I_{xx} + A_{44}} \quad (10)$$

We note here that the model under investigation did not have a cross-deck fitted during the experiments and the roll restoring would be under-predicted at angles where side hull top submergence occurs due to a significant decrease in the angle of vanishing stability. To properly account for roll damping at large angles of inclination, especially when a cross-deck is fitted on top of the outriggers, additional experiments will be carried-out and a non-linear restoring moment will be formulated by using a cubic or higher order polynomial, as follows:

$$C_{44}(\phi) = C_{44,1}\phi + C_{44,3}\phi^3 + [C_{44,5}\phi^5 + \dots] \quad (11)$$

The virtual mass moment of inertia includes the mass and added mass moments of inertia, which are calculated using the virtual displacement and virtual roll radius of gyration, as follows:

$$I'_{xx} = [(\Delta')/g]k_{xx}^2 \quad (12)$$

As shown by Bhattacharyya (1978), the added mass moment of inertia can be taken as a first approximation for being 20% of the mass moment of inertia, as follows:

$$I'_{xx} = \left[ \left( \frac{\Delta}{g} k_{xx}^2 \right) + \left( \frac{\delta\Delta}{g} k_{xx}^2 \right) \right] = [1.2\Delta/g]k_{xx}^2 \quad (13)$$

In the same reference, Bhattacharyya (1978) explained that based on many experiments carried-out for the determination of  $k_{xx}$  the accuracy of the added mass moment on inertia is less important considering its magnitude compared to that of the model itself.

The roll radius of gyration (in air) was computed experimentally from a swing test by using Eq. (14). During that test, the periods of oscillation in air were measured with a stop watch.

$$k_{xx}^2 = \frac{g}{(2\pi)^2} T^2 a - a^2 \quad (14)$$

An alternative estimate of the virtual added mass moment of inertia can be made using equation (15), by considering the linear portion of restoring moment at low to moderate angles of inclination and the small difference between the undamped roll natural frequency and the averaged (measured) damped roll natural frequency:

$$\omega_0^2 = \frac{\rho g V \cdot GM}{I_{xx} + A_{44}} \quad (15)$$

We should note that the added mass moment of inertia is frequency dependent and a function of the hull underwater geometry, which makes  $k_{xx}$  rather difficult to determine analytically. It can be calculated using seakeeping software, taken as a percentage of the mass moment of inertia or determined experimentally from a forced roll test.

The damping coefficients are derived, as shown by Himeno (1981), by integrating Eq. (7) over a half period and setting the energy dissipating by the roll damping equal to the work done by the restoring moment.

$$\Delta\phi = \pi k \phi_m + \frac{4}{3} \alpha \phi_m^2 + \frac{3\pi}{8} \beta \omega_0 \phi_m^3 \quad (16)$$

$$k = \frac{v}{\omega_0} \quad (17)$$

$$\Delta\phi = |\phi_j| - |\phi_{j+1}|, \text{ is the roll decrement} \quad (18)$$

$$\phi_m = \frac{|\phi_j| + |\phi_{j+1}|}{2}, \text{ is the mean roll angle} \quad (19)$$

The so-called extinction coefficients are extracted using a least squares regression fit as shown by Lewandowski (2004). This method will not provide a frequency dependence of roll damping but it will give an estimate of the damping coefficients. It allows us however to include and account for non-linearity in our linear model by defining an equivalent roll damping coefficient, as follows:

$$B_{44e}(\omega, \phi_0) = B_{44,1} + \frac{8}{3\pi} \omega \phi_0 B_{44,2} + \frac{3}{4} \omega^2 \phi_0^2 B_{44,3} \quad (20)$$

## ROLL DAMPING COEFFICIENTS

The extinction coefficients are obtained from third order regression analysis of decrement data as shown in Fig. 32-34. The linear, quadratic and cubic roll damping coefficients are calculated based on Eq. (8) and (16), which allow the equivalent damping coefficients to be determined based on Eq. (24). The coefficients are non-dimensionalized, as shown by Spouge (1988):

$$b_{44,1} = \frac{B_{44,1}}{2\omega_0(I_{xx} + A_{44})} \quad (21)$$

$$b_{44,2} = \frac{B_{44,2}}{2(I_{xx} + A_{44})} \quad (22)$$

$$b_{44,3} = \frac{\omega_0 B_{44,3}}{2(I_{xx} + A_{44})} \quad (23)$$

$$b_e = \frac{B_e}{2\omega_0(I_{xx} + A_{44})} \quad (24)$$

Table 3. Equivalent linear damping coefficients

Config.	RUN	FN	GM	$b_{44,e}$	Angle
C	175	0.00	44mm	0.07	6 Deg.
	286	0.16		0.19	
	288	0.24		0.38	
	291	0.32		0.50	
F	190	0.00	73mm	0.29	
	233	0.16		0.45	
	234	0.24		0.52	
	239	0.32		0.46	
I	194	0.00	108mm	0.18	
	231	0.16		0.26	
	228	0.24		0.32	
	209	0.32		0.44	

Table 4. Damping coefficients of 3<sup>rd</sup> order regression fit

Config.	RUN	FN	GM	$b_{44,1}$	$b_{44,2}$	$b_{44,3}$
C	175	0.00	44mm	0.07140	0.00002	0.00130
	286	0.16		0.18590	-0.00310	0.03070
	288	0.24		0.38970	0.00009	-0.00630
	291	0.32		0.50250	-0.00590	0.04150
F	190	0.00	73mm	0.30800	-0.00470	0.03770
	233	0.16		0.44860	0.00310	-0.02880
	234	0.24		0.49360	-0.00990	0.05570
	239	0.32		0.45600	-0.00440	0.02150
I	194	0.00	108mm	0.16130	0.00180	-0.00330
	231	0.16		0.20410	0.01050	-0.06050
	228	0.24		0.30940	0.00170	-0.00980
	209	0.32		0.45820	-0.00940	0.05390

The calculated non-dimensional roll damping coefficients corresponding to the same configuration and loading condition discussed previously are shown in Tables 3 and 4.

The linear damping coefficient  $b_{44,1}$  is obtained from the extinction coefficient  $k$  and represents a fraction of critical damping. We expect it to always be positive. A negative result cannot be interpreted physically and it could be an indication of poor high order regression fit to the data.

The quadratic and cubic damping coefficients  $b_{44,2}$  and  $b_{44,3}$  are derived from the extinction coefficients  $\alpha$  and  $\beta$ . The quadratic coefficient is expected to be positive, whereas the cubic term could be positive or negative.

The roll decay extinction curves for the aft most trimaran configurations *C*, *F* and *I*, are shown in Fig. 32-34. The first roll amplitude measured at the initiation of each roll decay test, and during which heave and pitch modes were coupled with their highest magnitude were removed from the analysis. As explained earlier, heave and pitch motions decay rapidly and have any significance during the first half of roll cycle (see Fig. 8). The corresponding distribution of non-dimensionalized linear, quadratic and cubic roll damping coefficients is shown in Fig. 35-37.

The damped roll natural frequency was not constant, which indicates that restoring moment was non-linear even at low to moderate inclination angles, especially for the outermost configurations. The damped roll natural period scatter of the aft most configurations *C*, *F* and *I* at their most stable loading

conditions shown in Fig. 38-40) indicate that the average period fluctuation is about 5%.

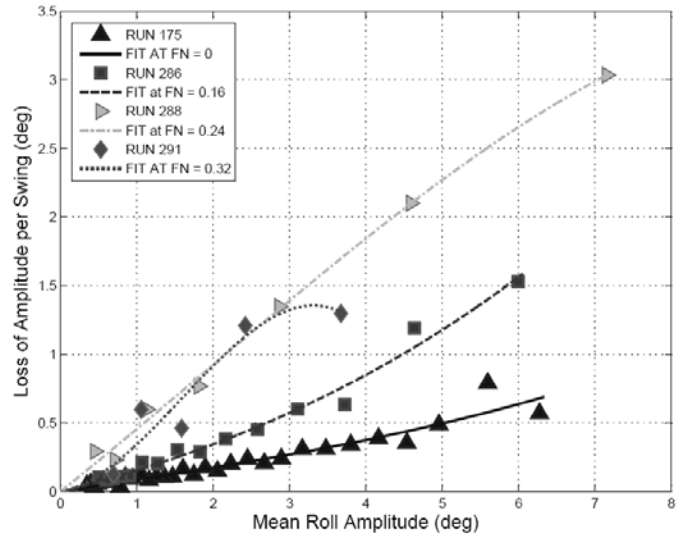


Fig. 32 Extinction scatter and regression; Config. C; GM = 44mm

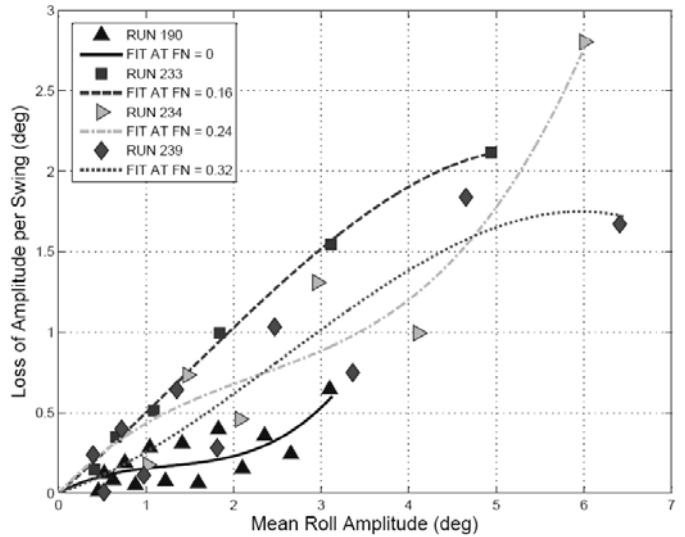


Fig. 33 Extinction scatter and regression; Config. F; GM = 73mm

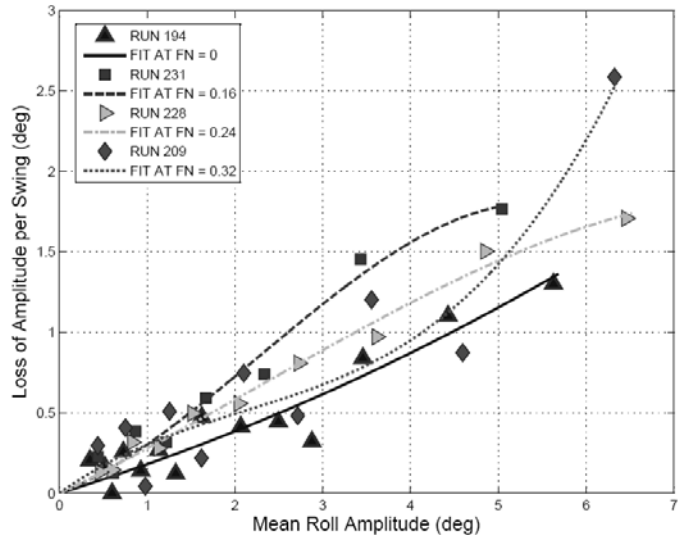


Fig. 34 Extinction scatter and regression; Config. I; GM = 108mm

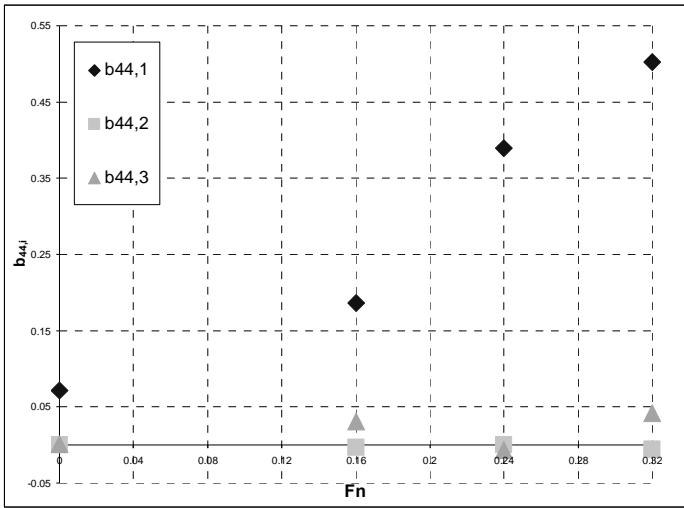


Fig. 35 Non-Dimensionalized Linear, Quadratic and Cubic Damping Coefficient for Config. C, GM = 44mm

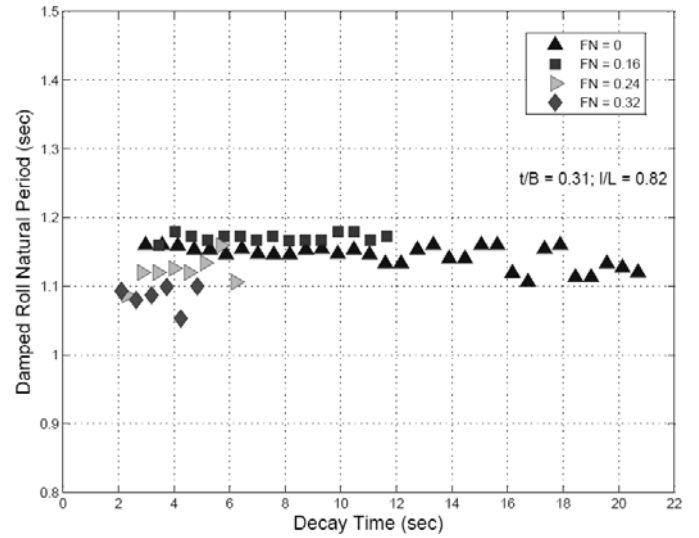


Fig. 38 Damped roll natural period scatter at GM = 44mm

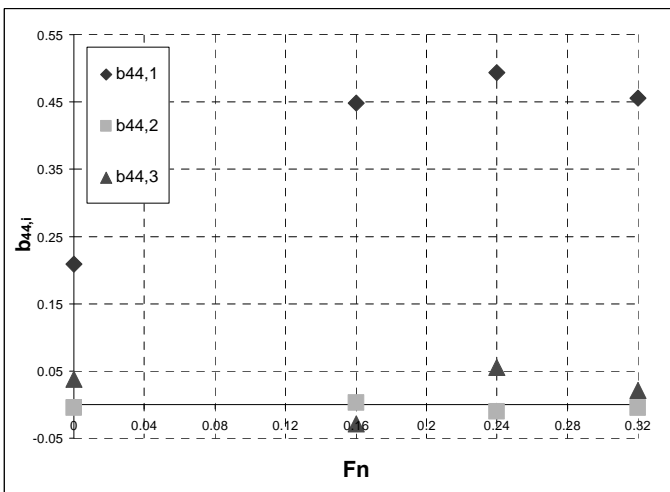


Fig. 36 Non-Dimensionalized Linear, Quadratic and Cubic Damping Coefficient for Config. F, GM = 73mm

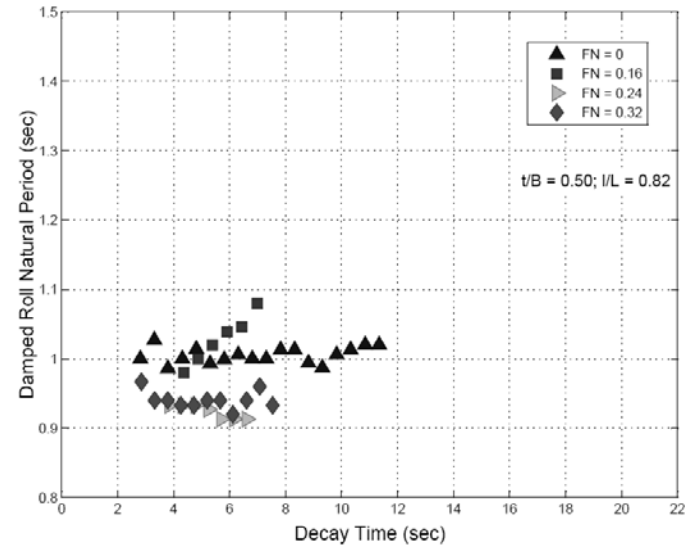


Fig. 39 Damped roll natural period scatter at GM = 73mm

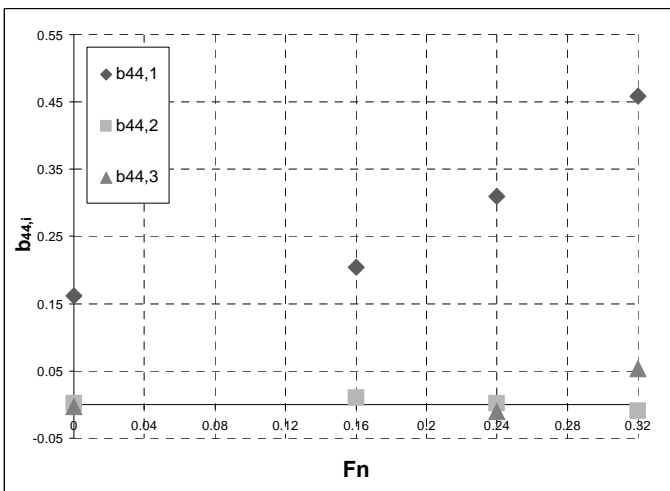


Fig. 37 Non-Dimensionalized Linear, Quadratic and Cubic Damping Coefficient for Config. I, GM = 108mm

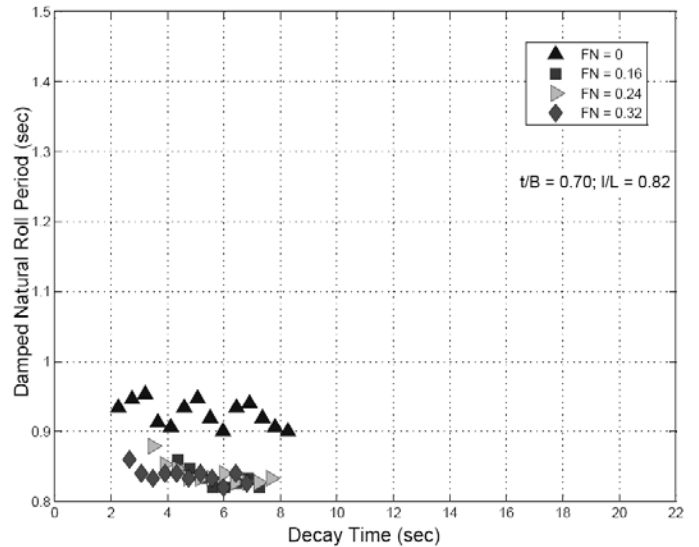


Fig. 40 Damped roll natural period scatter at GM = 108mm

It also illustrates the dependency of roll damped frequency on roll amplitude, as they both decreased throughout the roll decay time history, with the exception of one case at  $F_n = 0.16$  (Fig. 39). The implication of this observation is that linear restoring may not give accurate results unless is used for estimates at low inclination angles and the variation in natural frequency throughout the roll decay is small. The alternative solution is to use a non-linear approximation of the roll restoring moment. In a follow-up treatment the existing results of roll damping derived from roll decrement will be compared with results from alternative methods. Roll damping coefficients using energy methods were analyzed in previous research work published by Bass et al (1988), Grafton (2007), Roberts (1985), Spouge (1988) and Zhang et al (1999).

Once we establish that the equivalent roll damping coefficients are stable, the data will be used to solve numerically the differential equation of roll motion in order to determine the extent on which this roll damping model is suitable for predicting roll motions.

The data from the experiments for roll response in beam waves will be finally used to compare predicted results using seakeeping software, which will provide a final check on whether the existing roll damping model is suitable or it needs to be adjusted for trimarans.

## CONCLUSIONS

Results from three separate experiments on a trimaran model have been presented, free roll decay tests at zero and forward speed for nine different side hull spacing/stagger locations and roll response in beam seas for six of the nine configurations. The decay tests have been conducted at three speeds representative during the operation of the full scale frigate,  $F_n = 0.16, 0.24$  and  $0.32$ . The non-linear effects did not seem to dominate at zero to moderate speeds, as initially expected. The linear roll damping increased with speed as seen in other research studies.

The roll decrement analysis method was employed in the processing of the decay data, which was based on the work of Himeno (1981) and utilized a linear plus quadratic plus cubic expression of the roll damping moment. Although this type of analysis relies on proper regression fit of the data and is expected to show bias depending on the peaks and troughs removed from the decay, there was little negative scatter in the quadratic and cubic terms, which combined either provided a positive non-linear contribution to the total damping or it was very small in magnitude compared to the linear damping component. The quasi linear method for roll decay has not been utilized in this preliminary work due to its intrinsic high scatter of roll damping data and its strict dependency of damped roll natural frequency (Spouge, 1988).

The stability of the roll damping coefficients indicates that the trimaran bare hull (without fins or bilge keels) does not create highly non-linear roll damping. This is true provided the

outriggers are wall to near wall sided (as the model used in this experiment) thereby lacking the sudden increase in buoyancy, which would in turn create a heave damping moment with highly non-linear effects on both roll damping and restoring moments.

Extensive experimental studies on roll damping will be completed on the 1:80 scale version of the trimaran analyzed in this paper. The emphasis of that work will be comparing the roll damping coefficients with the smaller scale model's results as well as identifying the most suitable method for analyzing roll decay data for trimarans. Parametric roll instability will be studied at both scales using a free and a captive model setup. Numerical simulation of parametric roll will be carried-out using Det Norske Veritas' non-linear Rankine panel software WASIM, a 3-dimensional time domain potential flow program suitable for multihulls.

## ACKNOWLEDGEMENTS

This work is supported by the Office of Naval Research (ONR) under grant no. N00014-03-1-0160. The authors gratefully acknowledge the support of Ms. Kelly Copper, ONR program manager, and Dr. Colen Kennel, technical director of Center for Innovation in Ship Design (CISD), for providing the lines and engaging various discussions throughout the trimaran research program development.

The authors also wish to acknowledge the support of Det Norske Veritas for providing the non-linear ship motions software WASIM, which will be used throughout this research.

## REFERENCES

1. Bass, D.W. and Haddara, M.R. *Non-linear Models of Ship Roll Damping*. International Shipbuilding Progress, Volume 35, Issue 401, Pg. 5-24, 1988.
2. Belenky, V.L. and Sevastianov, N.B. *Stability and Safety of Ships – Risk of Capsizing*. The Society of Naval Architects and Marine Engineers, 2007.
3. Bhattacharyya, Rameswar. *Dynamics of Marine Vehicles*. John Wiley & Sons Inc., 1978.
4. Grafton, T. J. *The Roll Damping of Trimaran Ships*. Ph.D. Thesis, University College London, 2007.
5. Himeno, Y. *Prediction of Ship Roll Damping - State of the Art*. Report Number 239, Department of Naval Architecture and Marine Engineering, University of Michigan, Ann Arbor, Michigan, 1981.
6. Kat, J.O., Pinkster, D.J. and McTaggart, K.A. *Random Waves and Capsize Probability Based on Large Amplitude Motion Analysis*. Proceedings of OMAE 2002 21st International Conference on Offshore Mechanics and Arctic

Engineering, June 23-28, 2002, Oslo, Norway.

7. Lewandowski, Edward M. *The Dynamics of Marine Craft; Maneuvering and Seakeeping*. World Scientific Publishing Co., Pte., Ltd., 2004.
8. Oh, I.G., Nayfeh, A.H. and Mook, D.T. *A theoretical and experimental investigation of indirectly excited roll motion in ships*. Philosophical Transactions of the Royal Society of London, Vol. 358, Pg. 1853-1881, 2000.
9. Roberts, J. B. *Estimation of Nonlinear Ship Roll Damping from Free Decay Data*. Journal of Ship Research, Volume 29, No. 2, 1985.
10. Spouge, J. R. *Non-linear Analysis of Large-Amplitude Rolling Experiments*. International Shipbuilding Progress, Volume 25, Issue 403, Pg. 271-320, 1988.
11. Zhang, J. W.; Andrews, D.J. *Roll damping Characteristics of a Trimaran Displacement Ship*. International Shipbuilding Progress, Volume 46, Issue 448, Pg. 445-472, 1999.